Effects of loading conditions and specimen thickness on the flexural behavior of fiber-reinforced cementitious composites

Abstract

The flexural performance of polypropylene (PP) and polyvinyl alcohol (PVA) fiber reinforced cementitious composites (FRCC) have been investigated within the scope of this study. Thin plates and relatively thicker prismatic specimens have been prepared by using three fiber-matrix combinations. The center-point and two-point loading flexural performance of these specimens has been determined in terms of; first cracking strength, flexural strength and toughness. Test results showed that there is a significant difference in the flexural properties and toughness between thin specimens (mini-plates; thickness/span = 0.08) incorporating PP and PVA fibers. Despite their different shaped load-deflection curves, the flexural load carrying capacity of PP and PVA FRCCs was approximately same with the prismatic specimens (thickness/span = 0.31). According to center-point and two-point loading flexural test results, two-point loading condition seems more appropriate to visualize multiple cracking for PVA fiber reinforced thin members.

Keywords

fiber · flexural strength · multiple cracking · toughness

Burak Felekoğlu

Department of Civil Engineering, Dokuz Eylül University, Buca - İzmir, Turkey
e-mail: burak.felekoglu@deu.edu.tr

1 Introduction

Fiber reinforcement significantly improves the tensile performance of cementitious composites. Flexural loading tests are employed as an indirect and simple way of characterizing the tensile behavior of these materials. In general the performance of fiber reinforced cementitious composites (FRCC) under flexural load depends on many internal factors such as fiber material properties (e.g., fiber strength, stiffness, and Poisson's ratio), fiber geometry (smooth, end hooked, crimped, twisted), fiber dosage, matrix properties (e.g., matrix strength, stiffness, Poisson's ratio) and interface properties (adhesion, frictional and mechanical bond) [1, 2]. Furthermore, specimen size and loading conditions also affect the flexural response of FRCC [3]. In case of concrete, standard test method ASTM C1609 [4] has been widely used for determining flexural properties. Significant improvement in toughness and residual strength after first cracking is accessible by fiber reinforcement [5]. However, there is no universally accepted test method appropriate for fiber reinforced composites prepared by using very fine or even micro-aggregates. [maximum aggregate size $(D_{max}) < 1$ mm]. Two-point flexural loading test results on 120 x 30 x 10 mm and 355.6 x 50.8 x 76.2 mm specimens which were prepared with micro-aggregates have been previously reported [6, 7]. Nowadays high-performance FRCC with low D_{max} have been tested on specimens with various shapes and sizes [8, 9]. This variation in test conditions may cause difficulties in the interpretation and comparison of test results of different researchers. Comprehensive experimental studies on the flexural response of cementitious composites incorporating polymeric fibers and found that flexural performance significantly varies with the specimen geometry and loading conditions [9]. Specimen thickness and thickness/span ratio may significantly affect the flexural performance of cementitious composites. For example, the multiple cracking effectiveness of PVA based fibers in a cementitious matrix may differ significantly when flexural tests are performed on specimens with different thicknesses. This study aims to compare the effects of sample thickness and loading conditions on flexural response of polypropylene (PP) and polyvinyl alcohol (PVA) fiber reinforced cementitious composites.

There is a need to standardize the test methods, specimen shapes and sizes in order to compare various test results in case of FRCCs incorporating low D_{max} aggregate. The author believes that this study dealing with the flexural performance of fiber reinforced specimens at different thicknesses and loading conditions will be useful to understand the role of polymer-based fibers on flexural response.

2 Experimental Studies

Thin plate specimens [called as mini-plate: 10 x 60 x 170 mm] have been prepared by using a simple and effective specimen preparation method presented in this study. This method is suitable for the production of high volume fiber reinforced cementitious specimens ($\geq 2\%$ by volume). The flexural loading performances of these specimens were compared with relatively thicker standard prismatic specimens 40 x 40 x 160 mm conforming ASTM C 348 standard [10]. Additionally, the flexural resistances of thin plate specimens under center and two-point loading conditions were investigated. For this purpose, three fiber-reinforced composites (different matrices incorporating 2% PP and PVA fibers by volume) presenting distinctive load-deflection curves were used. These matrix-fiber combinations have been selected from a previous study [11].

2.1 Materials

An ordinary Portland cement (CEM I 42.5R) in conformity with TS EN 197-1 standard [12] and a C type of fly ash according to ASTM C618 [13] were used as the binder phase of composites. The chemical, physical and mechanical properties of these ingredients are presented in Table 1. Limestone powder with a maximum aggregate size (D_{max}) of 100 μm was used as the micro-aggregate phase. The specific gravity of micro-aggregate was 2.58. In order to improve the flowability of microconcretes a new generation polycarboxylate based superplasticiser with a solid content of 35.7% was also used. The pH and specific gravity of this superplasicizer are 6.5 and 1.18 respectively.

Three different polymer based fibers have been used in this research. The mechanical, elastic and surface structure properties of Polypropylene (PP) and two polyvinyl alcohol (PVA) based fibers are presented in Table 2. In order to illustrate the differences in surface roughness differences between the fibers, SEM images which have been captured at the same magnification, are also presented in Fig. 1. The polyolefin based polypropylene fibers are highly hydrophobic with a very smooth surface structure. Their tensile strength and modulus of elasticity are comparatively lower than PVA fibers. The different features of PVA (PVA-I & PVA-II) are also presented in Table 2. The rough surfaces of PVA fibers improve the mechanical interlocking (adhesion) capacity to the matrix. The mechanical properties of PVA fibers were almost equal to each other. As a geometrical difference, PVA-II is slightly thicker and longer than PVA-I (Fig. 1).

2.2 Matrix compositions and preparation of specimens

Three different mixtures by using two different matrices have been prepared based on the data taken from initial trial mixtures [11]. The binder phase of the first matrix was solely composed of cement (MI). PP fibers were incorporated into this high strength matrix. In the second matrix, 50% of cement was substituted with C type fly ash (MII). Due to highly reactive surface structure characteristic of PVA fibers, a high chemical bonding can be expected if a high strength matrix will be used. Extremely high chemical bond between a PVA fiber and matrix may result in a premature rupture of PVA fibers which decreases the multiple cracking capacity [6,9]. Due to this reason, MII matrix incorporating fly ash has been used to optimize the bonding and enhance multiple cracking behavior in case of PVA-I and PVA-II fibers usage. The fiber dosage was kept constant as 2% for all mixtures (Table 3). These fiber-matrix compositions have distinct flexural behaviors for each fiber type.

Mixing sequence was kept constant for all mixtures. Cement and fly ash in the case of second matrix were dry mixed for 30 sec in a 5 lt capacity planetary mortar mixer conforming ASTM C 305 requirements [14]. This mixer is manufactured by a regional supplier (Unal Muhendislik & Makina San). After the addition of water and superplasticizer, mixing was continued for a period of two minutes. Finally, fibers were added to the wet mixture and mixing was prolonged to an extra 4 min. This additional mixing is performed to activate the polycarboxylate molecules and improve the fibers dispersability [9]. Flow diameters of mixtures prepared by using MI and MII matrices are presented in Fig. 2.

Mini-plate specimens were prepared by using zipped nylon bags. The specimen preparation stages have been illustrated in Fig. 3. The volume of each specimen was kept constant by using a 100 cm^3 volume mica pot. The mixture was poured and compacted into this pot (Fig. 3 (a)). Then the mixtures were poured into the nylon bags (Fig. 3 (b)). The bags were sealed after the discharge of air (Fig. 3 (c)). The zipped bags were laid down on a flat surface and their top surface is leveled parallel to surface by using a glass plate and a spirit level (Fig. 3 (d) - 3 (e)). Plate specimens' thicknesses were reduced to 10 mm. The length and width were also kept constant as 170 mm and 60 mm respectively (Fig. 3 (f) - 3 (g)). Nylon bags were torn one day after casting and the specimens were cured in water for 28 days until testing. Same mixtures were also cast into 40 x 40 x 160 mm prismatic molds conforming ASTM C348 standards for comparison [10]. Three specimens were prepared for each mixture. Prismatic specimens were demolded one day after casting and standard cured in lime saturated water for 28 days.

2.3 Flexural tests

The flexural tests have been performed by using a close loop deflection controlled machine. The rate of deflection was kept constant as 0.2 mm/min. and the span was 130 mm for all loadings. 40 x 40 x 160 mm prismatic specimens and

Tab. 1. Physical and chemical compositions of Portland cement and fly ash.

Oxide Composition (% by weight)		CEM I 42.5R	Type C fly ash
CaO		63.70	26.96
SiO_2		19.14	42.14
Al_2O_3		5.75	19.38
Fe_2O_3		3.00	4.64
MgO		0.90	1.78
Na_2O		0.65	-
K_2O		0.83	1.13
SO_3		2.78	2.43
Compressive Strength (MPa)	2 days	20.4	-
	7 days	41.1	-
	28 days	50.6	-
Specific gravity		3.12	2.20
Blaine SSA (m^2/kg)		336	290
Volume expansion (mm)		1	-
Consistency water (%)		28.8	-
Initial setting time (min.)		135	-
Final setting time (min.)		245	-

Tab. 2. Physical and mechanical properties of fibers.

Fiber type	Density, kg/m^3	Diameter, μm	Length, mm	L/D ratio	Tensile Strength, MPa	Elongation at failure, (%)	Modulus of elasticity, GPa	Cross section form	Surface structure
Polypropylene (PP)	950	40	12	300	400-550	> 30	5.6	Circular	Smooth
Polyvinyl alcohol (PVA-I)	1300	26	6	230	1600	6	39	Circular	Rough
Polyvinyl alcohol (PVA-II)	1300	30	8	200	1600	6	42	Circular	Rough

Tab. 3. Mixture proportions of selected matrices.

Matrix code	Mixture Ingredients, kg/m^3				Superplasticizer dosage (% by weight of binder)	Fiber dosage (% by volume of matrix)
	Cement	Water	Fly ash	Limestone powder		
MI-PP	854	380	0	854	1.2%	2%
MII-PVA-I	378	399	378	757	1.4%	2%
MII-PVA-II	378	399	378	757	1.4%	2%
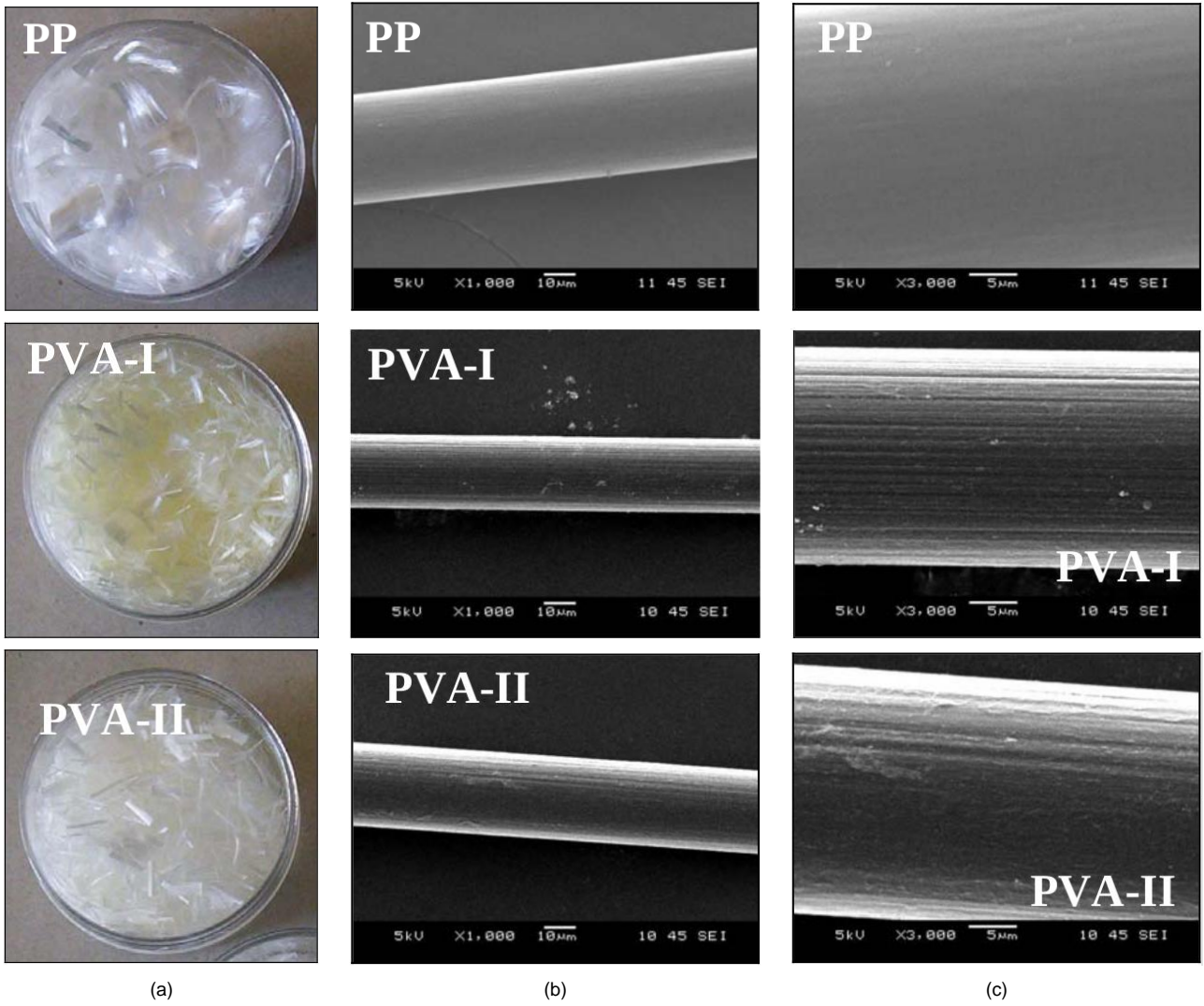
Fig. 1. Bulk photos (a) and scanning electron microscope images of magnifications. polypropylene and polyvinyl alcohol based fibers at 1000x (b) and 3000x (c)

| PP %2 – matrix MI | PVA-I %2 – matrix MII | PVA-II %2 – matrix MII |
| 165 mm | 154 mm | 128 mm |
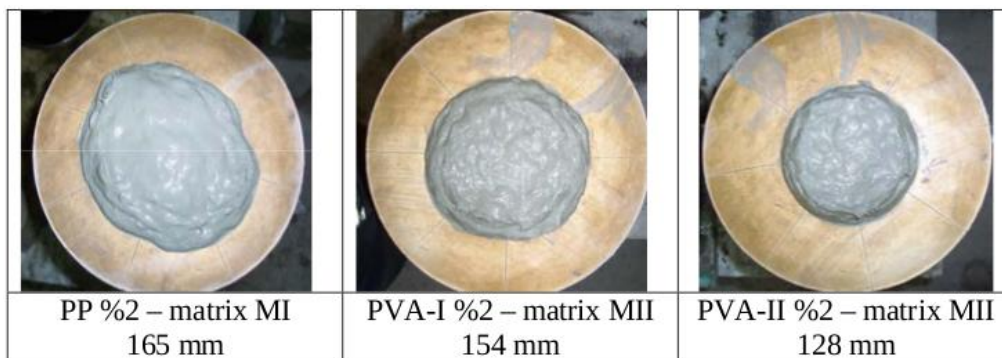
Fig. 2. The flow diameters of mixtures after tilting on the flow table.
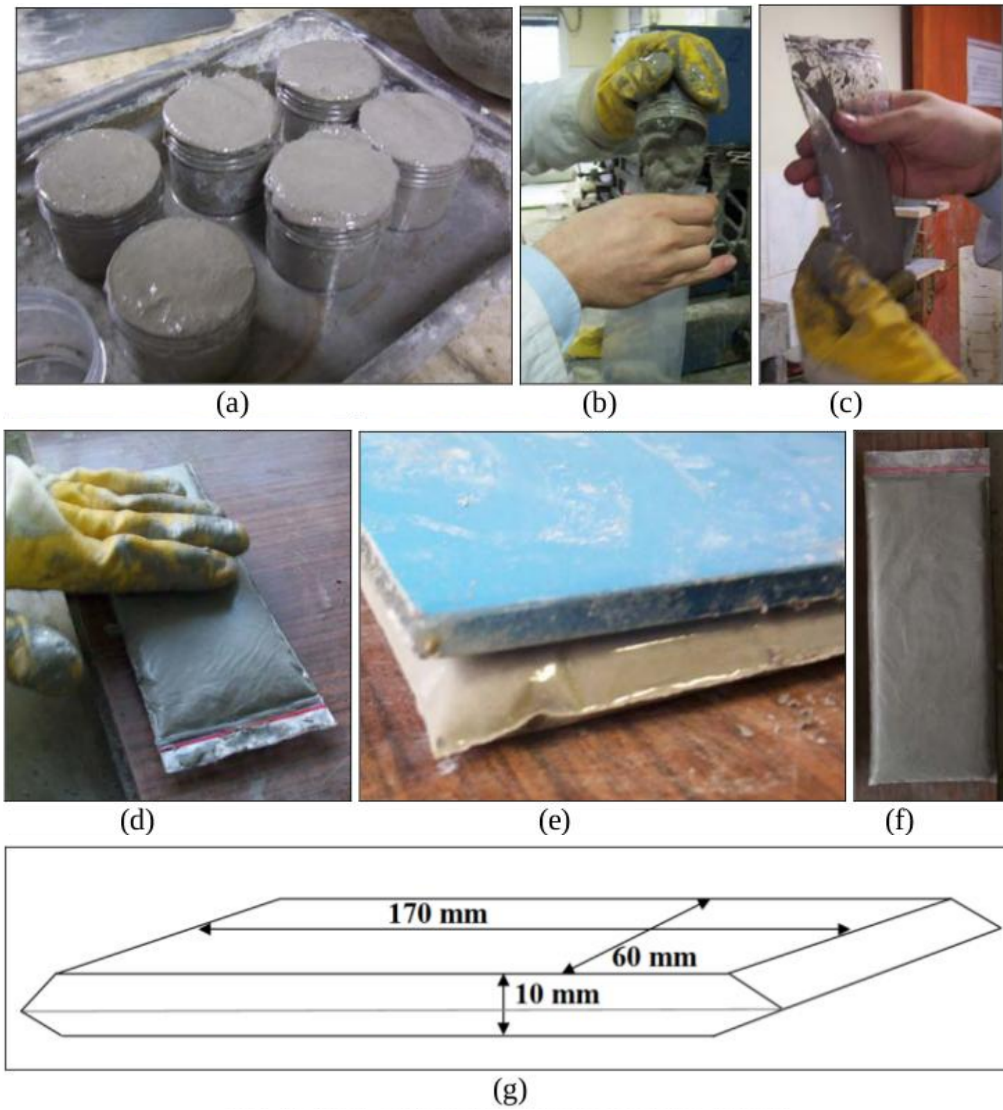
Fig. 3. Mini-plate specimen preparation stages.

10 x 60 x 170 mm mini-plates were tested under center-point loading (Set-A and Set-B respectively). The thickness/span ratios of these specimens were 0.31 and 0.08 respectively. Mini plate specimens were also tested under two-point loading (Set-C). The illustrations of loading conditions are also presented at each of load-deflection graphics. Load-deflection data up to 2.5 - 3 mm of deflection was recorded for 40 x 40 x 160 mm prismatic specimens. In case of 10 x 60 x 170 mm mini-plates, load-deflection data was recorded up to 4.5 mm deflection value (Fig. 4).

It should be noted that, if the ratio of loading span length to width is lower than 2, specimens behave like a "plate". In practice the plate behavior is more complex compared to a simple beam behavior. In this case, the ratio of loading span length to plate width is 2.17. Due to this reason these specimens behave as "shallow beam" [11]. However, these specimens look like a plate rather than a "shallow beam" and were named as "mini-plate".

3 Results and Discussion

The load – deflection behavior of all specimens are illustrated in Fig. 4. The center-point load-deflection curves of 40 x 40 x 160 mm prismatic specimens (Set-A) and mini-plates (Set-B) are presented in the first and second rows, respectively. The two-point loading curves of mini-plates can be seen in the last row (Set-C). The load carrying capacities of prismatic specimens with 40 mm thickness were extremely higher than mini-plate specimens [10 mm thickness]. For this reason, different y-axis scales have been chosen for the graphics. The flexural test data (first cracking load, maximum load after first cracking and mid-point deflection at these loads, flexural strength and toughness) are also presented in Table 4. The first sudden drop at the flexural load carrying capacity was accepted as the first cracking point (e.g. indicated in Fig. 4 (a)). In case of a continuous slope change at the initial linear part of load deflection curve, first cracking point has been determined by prolonging two tangents from the linear portions of curves. The vertical intersection point with the curve was accepted as the first cracking point. Flexural strength values have been calculated by using the maximum load at the deflection capacity (e.g. indicated in Fig. 4 (a)). In general, the maximum load was higher than the first cracking load in almost all cases. The flexural toughness values of all specimens have been calculated by integrating the area under the load-deflection curves up to 1/100 of span (1.3 mm).

Control specimens of 40 x 40 x 160 mm (without any fiber addition) were also subjected to center-point flexural test for comparison purpose (Set A). Related test data is presented in Table 4. A sudden collapse with a single cracking has been observed in all these specimens which indicates brittle flexural behavior. The toughness and flexural strength values of plain specimens were relatively lower than the specimens incorporating PP and PVA fibers.

In general, fiber reinforcement improved the load carrying capacity of specimens at higher deflection values. However, the magnitude of flexural load carrying capacity at any deflection value is significantly different depending on the fiber and loading conditions (Fig. 4, Table 4). Due to this reason, discussions have been performed on fiber-type basis.

3.1 PP fiber reinforced specimens

In case of PP fiber reinforcement, there is a linear part in the load – deflection curve of 40 x 40 x 160 mm specimens (Set-A, Fig. 4 (a)). A sudden crack formation and a large deflection was measured around 3550 N. At this point, a load drop with a magnitude of approximately 2000 N was observed. Following this load drop, fibers bridged the initial crack and regain flexural load carrying capacity by both stretching and elongation. During crack propagation, new fibers at the upper zone of the cracking plane activated and increased the load carrying capacity of the composite. This behavior continued until the midpoint deflection of about 0.65 mm where maximum load has been measured. The load at this deflection value was higher than the first cracking load. High volume fraction of PP fibers (2% by volume) showed an enhancement of flexural strength as previously reported by [15]. Above this point, the flexural load carrying capacity of the composite decreased due to the excessive fiber slippage from the matrix. The smooth surface of fibers is responsible for the slippage and the slipped portions of fibers can be observed at the crack openings. At higher deflection values some fibers completely slip off and detached from the matrix. As the fibers located near the bottom lost their load carrying capacity by detaching, composite's performance decreased. However, this drop progressed rather slowly due to the high elongation capacity of PP fibers. It should be noted that, a single crack was formed at all specimens and this crack widened until the end of testing. No other crack was observed on the bottom surfaces of the specimens.

When the mini-plate specimen is subjected to center-point loading, generally similar behavior that explained in previous paragraph was observed with some exceptions (Set-B, Fig. 4 (d)). Even though, the load drop pattern after the first crack was proportionally similar to the case in Set-A, the load gain due to fiber bridging never exceeded the first crack loading values. In this context, the first cracking strength can be accepted as flexural strength of these composites. The fiber elongation and slippage from the matrix with a reduced load governed the general behavior after the first cracking. Results indicated that, PP fibers were not effective in matrix bridging and load gaining at higher deflection ratios in the case of mini-plate specimens. Note that PP fibers were effective in load regaining if employed in thicker composites. The maximum load after first cracking was considerably higher for thicker specimens as seen in Figs. 4 (a) and 4 (d). As a possible conclusion, relatively low number of fibers at a cross section reduced the performance of these low-strength fibers in case of thinner composites. Single cracking

(a) (b) (c)

(d) (e) (f)

(g) (h) (i)
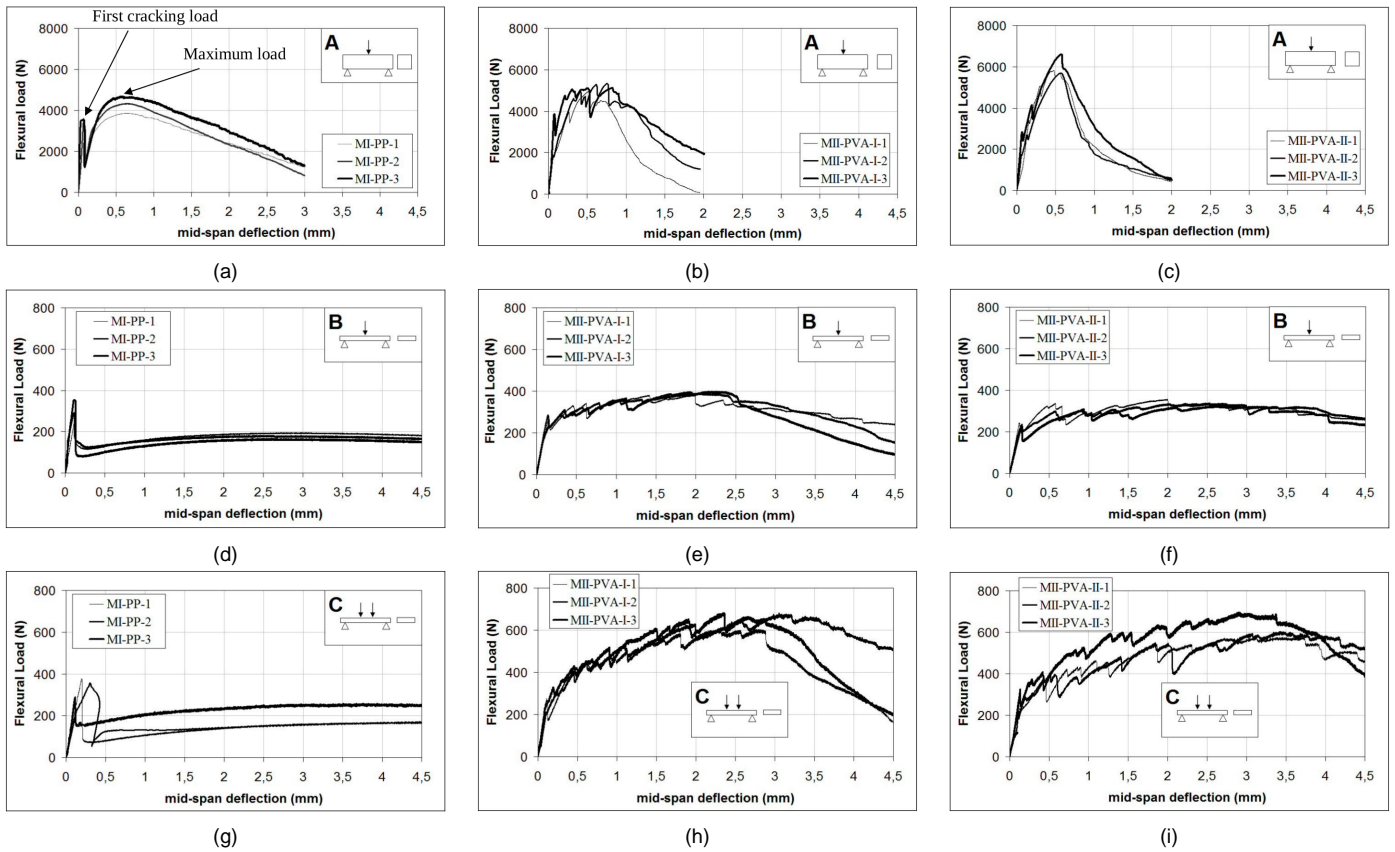
Fig. 4. The load – deflection behavior of specimens at different loading conditions:

a,b,c: Set-A [40 x 40 x 160 mm center-point loading],

d,e,f: Set-B [10 x 60 x 170 mm center-point loading],

g,h,i: Set-C [10 x 60 x 170 mm two-point loading].

Tab. 4. Flexural strength test results.

Loading Type	Specimen Code	First cracking load	First cracking deflection	Maximum load after first cracking	Deflection capacity	Flexural Strength*	Flexural Tough-ness**
		(N)	(mm)	(N)	(mm)	(MPa)	(N.mm)
A	MI-0	3120	0.087	-	-	9.5	210
	MII-0	2390	0.063	-	-	7.3	90
	MI-PP	3550	0.080	4266	0.646	13.0	4810
	MII-PVA-I	2512	0.061	5127	0.702	15.6	5015
	MII-PVA-II	2650	0.093	5991	0.550	18.3	4593
B	MI-PP	294	0.110	181	2.638	9.6	179
	MII-PVA-I	247	0.131	386	1.935	12.5	384
	MII-PVA-II	233	0.142	335	2.236	10.9	329
C	MI-PP	295	0.150	198	4.087	6.4	208
	MII-PVA-I	240	0.105	655	2.722	14.2	516
	MII-PVA-II	254	0.112	624	3.358	13.5	483

* Flexural strength: $\sigma_{center\ point\ loading} = \frac{1.5PL}{bh^2}$ $\sigma_{two\ point\ loading} = \frac{PL}{bh^2}$,

P: Maximum load, L: length of the support span, b: width, h: thickness

** Flexural toughhness: The area under the load deflection curve up to 1/100 of support span length (1.3 mm)

and slippage of fibers along this cracked section can be observed in Fig. 5. The behavior of mini-plates in the case of two-point loading was nearly similar to the ones observed in center-point loading only with an exception of variability in load-deflection curves. The flexural load carrying capacity never reached to the values obtained just before first cracking (Fig. 4 (g)). Due to this reason, the first cracking and flexural strength of these specimens were similar.

In order to investigate the fiber pull out behavior small particles have been manually detached from the sides of crack openings of PP reinforced mini-plate specimens. These specimens were investigated by using a scanning electron microscope (SEM) and photographs have been captured at different magnifications (Fig. 6). As seen in Fig. 6 (a), the detached lengths of PP fibers from the matrix were longer than 4 - 5 mm which was the indication of excessive fiber slippage. Other observations that indicate fiber slippage from the matrix can be listed as; presence of holes at the opposite side of a detached fiber from the matrix, a longitudinal trace of detached fiber on the matrix (Fig. 6 (b)) and formation of voids at the interface between slipped fibers and matrix (Fig. 6 (c)). All these microstructure observations confirmed that in case of thin-plates PP fibers are not suitable for matrix bridging efficiency.

3.2 PVA fiber reinforced specimens

The load – deflection curve of 40 x 40 x 160 mm specimens incorporating PVA-I fibers is presented in Fig. 4 (b) (Set-A). The first cracking load was in the order of 2000 - 4000 N (Fig. 4 (b)). After the first crack, additional multiple cracks formed around the mid-span of specimens. Due to the high frictional bond between rough surface of PVA fibers and the matrix and high tensile strength of PVA fibers, the flexural load carrying capacity of composite has improved. A further improvement even at higher deflection values has been provided by the optimized chemical bond between PVA fibers and matrix incorporating fly ash. Each new formed crack results in a sudden load drop and a following load gain. This situation can be observed on load deflection curves of some specimens as a "zig zag" form structure. Multiple cracking improved the flexural load carrying capacity of composites up to a certain deflection value. The increase in load-carrying capacity at increasing flexural deflection values indicates that composites are presenting a deflection hardening or pseudo-strain hardening behavior. On the other hand 40 x 40 x 160 mm specimens incorporating PVA-II fibers showed a higher flexural strength at center-point loading (Fig. 4(c), Set-A). The ascending and descending sections of load deflection curves are comparatively steeper and sharper than the case of PVA-I fibers. This behavior can be attributed to the relatively quick rupture of PVA-II fibers at comparatively higher loading levels. Smaller diameter and shorter length of PVA-I fibers compared to PVA-II fibers increase the number of fibers per unit volume of matrix when fibers used at equal volumetric dosages. Due to the lower number of PVA-II fibers at

a crack opening, stress may be localized heterogeneously and fiber rupturing took place earlier compared to the PVA-I fiber reinforced composites.

In case of Set-B, PVA fiber reinforced mini-plate specimens have been tested under center-point loading. The load-deflection curves of PVA-I and PVA-II fiber reinforced composites have been presented in Figs. 4 (e) and 4 (f) respectively. The shape of the curves indicated that multiple cracking behavior after the first crack was also apparent for this loading case. The maximum average load has been obtained at relatively higher deflection values. The deflection hardening behavior was noticeable and the flexural load carrying capacity was increased from 250 N to about 400 N at 2 mm of mid-span deflection (Figs. 4 (e) and 4 (f)). The number of visible cracks around the mid-span increased during this period (Fig. 7). These results showed that thin plate composites incorporating PVA fibers were also providing their multiple cracking behavior under center-point loading. Strong and high modulus PVA fibers have the ability to bridge matrix cracks and distribute the stresses to the other parts of matrix structure even in the case of thin cross sections. The optimized chemical bond between PVA fibers and matrix incorporating fly ash is the main cause of enhanced multiple cracking behavior up to a definite deflection capacity.

The load-deflection curves of the last set of PVA fiber reinforced specimens (Set-C) subjected to two-point loading has been presented in Figs. 4 (h) and 4 (i), respectively. In this loading type, one-third of the span in the middle is subjected to a constant flexural moment value and there is no shear force in the middle region. The two-point loading condition further increased the numbers of multiple cracks and shifted the curves of both PVA fibers upwards. The flexural load carrying capacity of specimens increased [up to 600 ~ 650 N] and the deflection hardening behavior was noticeable around 3 - 3.5 mm deflection values. The visible multiple cracks (> 30) were distributed on the specimen in the middle region (Fig. 8 (c)). After the formation of first crack, the bridging PVA fibers stretched between two adjacent sides at the crack opening. PVA fibers resist higher stress levels and effectively distribute the load to other sections of specimens with a very slight slipping. At higher stress levels multiple cracks randomly formed at weaker zones of the specimen. The formation of each new crack helps to relieve the stress level at bridging fibers of former cracks. By this way flexural load carrying capacity can be sustained and/or improved at the increasing deflection values (deflection hardening behavior). Some of these fine cracks exhibit a type of semi-elastic behavior. The widths of these fine cracks were about 50 - 100 microns. If the composites are unloaded at this stage, crack openings tend to close due to the elastic recovery response of bridging fibers. This mechanism is valid up to the deflection capacity. After a certain deflection limit, a major single crack widens, where bridging PVA fibers at this crack zone begin to rupture (stress level exceeded the strength of fibers). Instantaneously, other cracks begin to close up due to the stress relief in bridging fibers
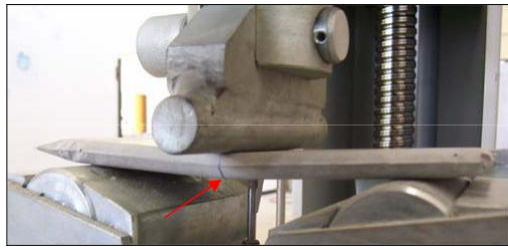
Fig. 5. Single cracking and slippage of PP fibers observed in cracked section and slippage of PP fibers from the matrix.
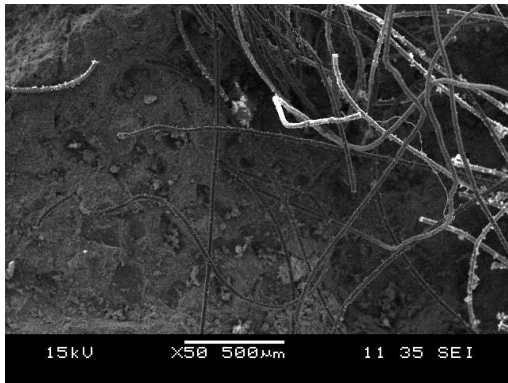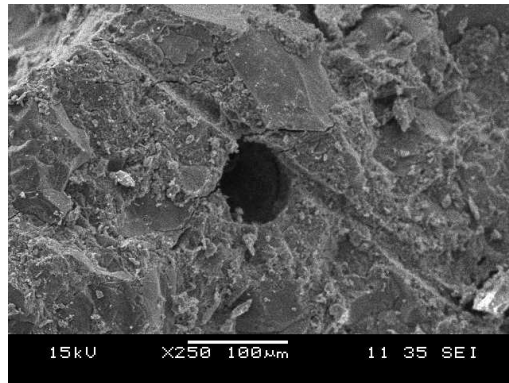
Fig. 6. SEM images of particles detached from mini-plate incorporating 2% PP fibers.
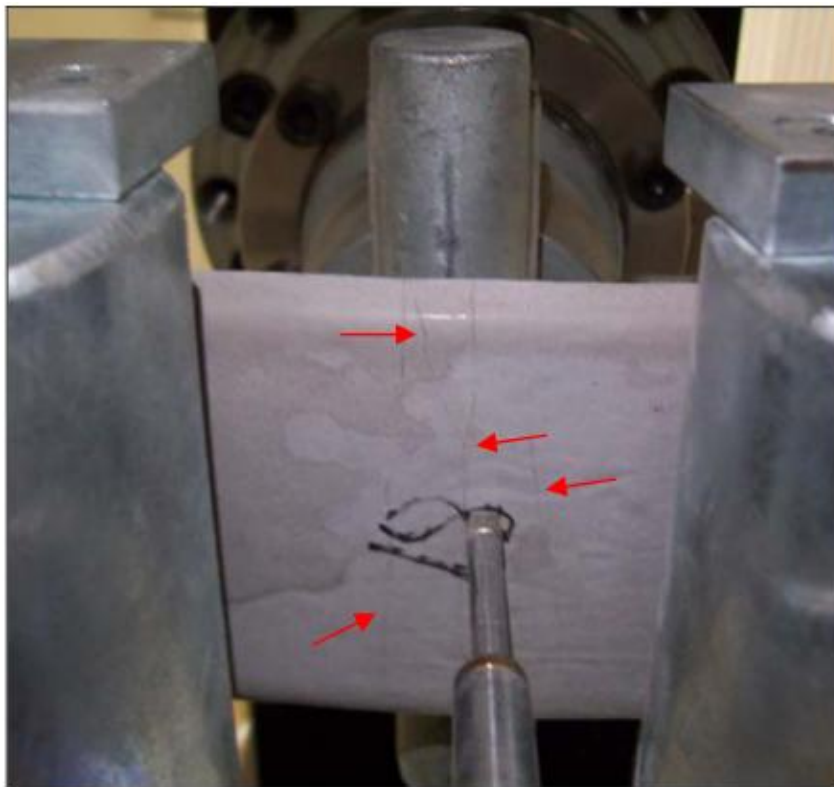
Fig. 7. Multiple cracking observed in thin-plate specimens incorporating PVA-I fibers under center-point loading (Set-B).

at their crack openings. Specimen surfaces were painted for better observation of multiple cracks (Fig. 8 (c)).

In order to clarify the effect of PVA fibers in collapse mechanism, two small particles have been detached from the cracked specimen (incorporating PVA-I fibers), seen in Fig. 8 (c). Inner structures of these specimens were investigated by using a scanning electron microscope (SEM). There are two semi-elastic cracks (which closed upon unloading) on the first particle (Fig. 9(a)). When one of these cracks is closely investigated, the matrix bridging PVA-I fibers were detected (Fig. 9 (b)). The crack widths along this crack varied between 50 - 100 microns. High strength PVA fibers with rough surfaces bridging the matrix by friction and distributing the stress to the other parts of the matrix are responsible to the formation of new parallel cracks at other cross sections of mini-plate specimens. Note that, in the case of PP fiber reinforced thin-plate specimen, fibers were debonded and started to strip out at comparatively lower stress levels due to their low frictional bond with the matrix. Second particle has been taken from the major crack cross-section of the thin-plate specimen following flexural test (Fig. 8 (c)). The SEM image of this piece clearly showed that "rupture" is the main collapse mechanism of these fibers rather than significant slippage and pull-out (Fig. 9 (c)). It was reported that in addition to surface roughness the chemical bonding capacity of PVA fibers with cementitious matrices are responsible for this relatively high bond strength [16].

3.3 Comparison of fiber performances at different specimen thicknesses and loading conditions

The flexural capacity of PP fiber reinforced composites with a high strength matrix and two PVA fiber reinforced composites in combination with a matrix incorporating fly ash have been compared at high fiber dosages (> 2%). Results showed that the maximum load carrying capacity (after initial crack) and flexural toughness values of investigated matrix-fiber combinations are comparatively similar if thicker specimens have been used in flexural testing. There is only ± 5% difference between the flexural toughness values of thick specimens incorporating PP and PVA fibers as seen in Fig. 10 (Set A). On the other hand, in case of thin specimens, the flexural toughness of specimens with PVA fibers was two times higher compared to PP fibers. The magnitude of improvement is more significant if loading condition is converted to two-point rather than center-point loading (148% and 132% improvement for PVA-I and PVA-II fibers respectively).

The effect of specimen thickness on the performance of PP and PVA fibers can be attributed to the following mechanism: Relatively thick specimens contain more fibers at the maximum stress zone compared to thinner specimens. During the initiation of first crack, existence of large number of fibers bridges the matrix as a result of extreme fiber dosage (2% by volume). These enormous numbers of fibers distribute the load at lower stress levels. The type of fiber is a minor factor in this case.

Low strengths and smooth surfaces of PP fibers are not vulnerable factors for thick sections if used at extremely high dosages. However, at the maximum stress zones of thin and flat specimens (bottom) there are fewer fibers even at high dosages of fiber usage. In this case, the strength of weak PP fibers will never be sufficient to increase the flexural load carrying capacity. On the other hand, PVA fibers were stronger and bonding ability with cementitious matrix is better compared to PP fibers. Despite their limited number at the cracked section, these fibers were capable of distributing the stresses and form multiple cracking throughout the specimens. The deflection hardening response of PVA fiber reinforced composites even at thin specimens is due to increase of number of active bridging fibers by the formation of new extra parallel cracks. Generation of each new crack activates many new load bridging fibers at these parallel cracks [17, 18]. This deflection hardening response can be observed as the deflection increases up to a limited value. As indicated before, if chemical bond between fiber and matrix is optimized by using fly ash, the deflection capacity of PVA fiber reinforced composites can be further improved. After this limit the stress on PVA fibers exceed their tensile strength and rupture takes place. Similar results with relatively thin specimens [120 x 30 x 10 mm] incorporating PVA fibers have been reported by [6].

In case of conventional concrete specimens, flexural test results obtained from different loading conditions can be interpreted as follows: If center-point loading test is applied, failure occurs when the tensile strength of concrete at the bottom section under the loading point is exhausted. On the other hand, under third-point loading, one-third of the length of the extreme fiber in the beam is subjected to the maximum stress, so that the critical crack may develop at any section in one-third of the beam length. Because the probability of a weak element (of any specified strength) being subjected to the critical stress is considerably greater under two-point loading than when a central load acts, the center-point loading test gives a higher value of the flexural strength value (Neville, 2000) However, this is not the case for PVA fiber reinforced cement-based composites and the effect of loading conditions on flexural performance is significantly different. Under two-point loading conditions, the uniform flexural moment values in the mid-region both improved the multiple cracking response and flexural strength of composites due to the superior bridging performance of PVA fibers up to significant deflection values.

The flexural performance of concrete is important for many current applications such as overlays for highways, bridge decks, slab and airport pavements repairs, roofing tiles and partition walls [20, 21]. In most cases, application depths are limited and relatively thin sections are required. PVA fiber reinforced composites specially designed with a proper matrix combination as presented in the above sections are potentially suitable and their employment can be an effective solution for these kinds of applications.

(a)   (b)

(c)
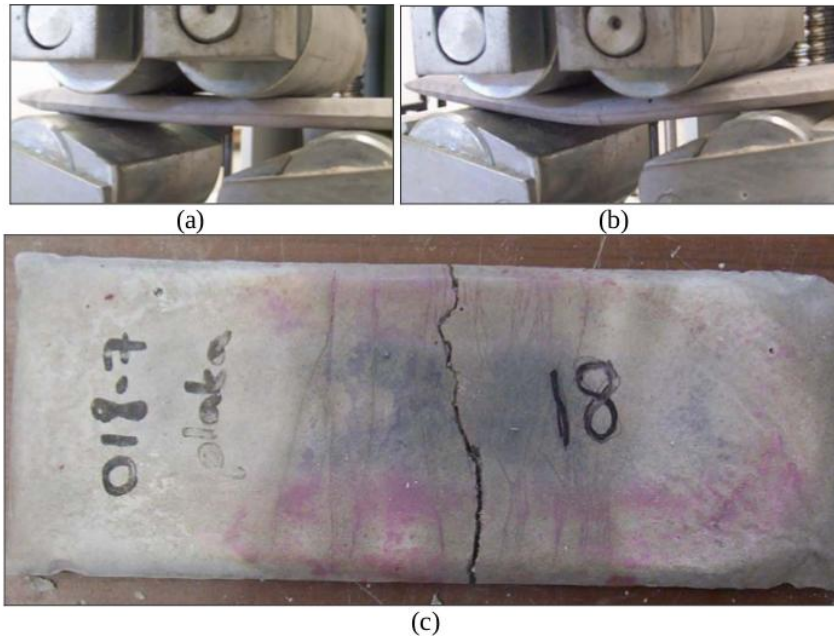
Fig. 8. Multiple cracking observed in thin-plate specimens incorporating PVA-I fibers under two-point loading (Set-C). a) Before loading, b) Main crack formed under loading at extreme deflection values, c) Multiple cracks closed after the formation of main crack.

(a)   (b)   (c)
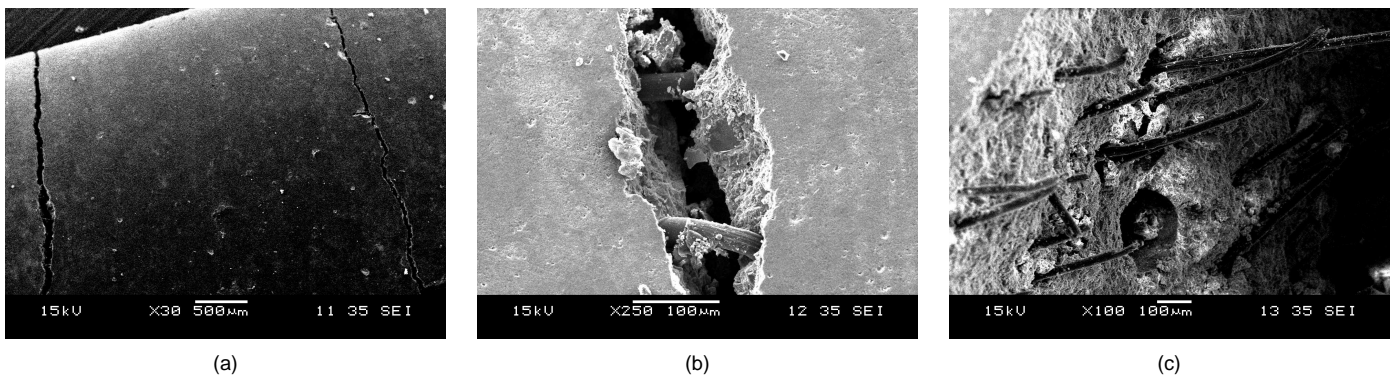
Fig. 9. SEM images of particles detached from mini-plate incorporating 2% PVA-I fibers. a) Semi-elastic parallel cracks on specimen, b) Closer look into a crack opening, c) Fibers ruptured at the end of flexural testing.
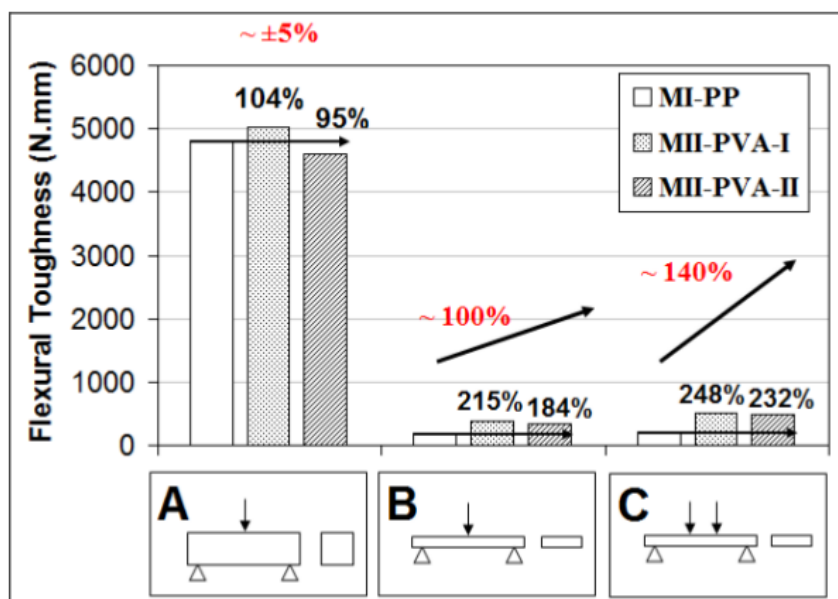
Fig. 10. Effects of specimen thickness and loading mode on flexural toughness of fiber reinforced composites.

4 Conclusions

The flexural behavior of three polymer FRCC specimens at two different thicknesses under different loading conditions has been studied in detail and the following conclusions have been derived:

1 In case of thick specimens (prismatic; thickness/span = 0.31), the fiber bridging capacity of PP fibers in a strong matrix is comparatively similar to the multiple cracking performance of PVA fibers in fly ash incorporated matrix in terms of "flexural load carrying capacity after first cracking load" and "flexural toughness".

2 There is a distinct performance difference between the flexural load carrying capacity and toughness of thin specimens (mini-plates; thickness/span = 0.08) incorporating PP & PVA fibers. While the fiber bridging performance of PP fibers was insufficient in case of mini-plates, the multiple cracking responses of PVA fiber incorporated specimens were impressive. The main cause of this performance may be the optimized chemical bonding between PVA fibers and matrix by incorporation of fly ash. It may be concluded that, PVA fibers can be efficiently used in thin members such as thin-slab applications due to their high strength and multiple cracking response in a proper matrix.

3 The center-point and two-point loading tests performed on PVA fiber reinforced thin-plates showed that multiple cracking performance of PVA fibers improves if the load applied in a more uniform manner. Under two-point loading conditions, the uniform flexural moment values in the mid-region both improved the multiple cracking response and flexural strength of composites due to the superior bridging performance of PVA fibers up to significant deflection values. Two-point loading condition seems more appropriate for determining the flexural strength and toughness of PVA fiber reinforced thin members compared to center-point loading. On the other hand, no significant flexural performance difference was observed by changing the loading condition in the case of PP fiber reinforcement.

4 Although the number of data obtained from this study is limited; it can be recommended that, using shallower beam test specimens is more appropriate in order to characterize the multiple cracking potential of a specific fiber in fiber reinforced cementitious composites incorporating fine and micro-aggregates.

References

1 **Kim DJ, Naaman AE, El-Tawil S**, *Comparative flexural behavior of four fiber reinforced cementitious composites*, Cement and Concrete Composites, **30**(10), (2008), 917–928, DOI 10.1016/j.cemconcomp.2008.08.002.

2 **Aydın S**, *Effects of fiber strength on fracture characteristics of normal and high strength concrete*, Periodica Polytechnica Civil Engineering, **57**(2), (2013), 191-200, DOI 10.3311/PPci.7174.

3 **Mechtcherine V, Schulze J**, *Effect of the test set-up and curing conditions on fracture behavior of strain hardening cement-based composites (SHCC)*, International Symposium on Measuring, Monitoring and Modeling Concrete Properties, In: **Konsta-Gdoutos M** (ed.), Measuring, Monitoring and Modeling Concrete Properties, Springer; Northwestern University, USA, 2006, pp. 33–39, DOI 10.1007/978-1-4020-5104-3_4.

4 *ASTM C 1609: Standard Test Method for Flexural Performance of Fiber-Reinforced Concrete (Using Beam With Third-Point Loading)*, ASTM International; 100 Barr Harbor Drive, PA, United States, 2012.

5 **Erdelyi A**, *The toughness of steel fibre reinforced concretes*, Periodica Polytechnica Civil Engineering, **37**(4), (1993), 329–344.

6 **Zhou J, Qian S, Beltran M, Ye G, van Breugel K, Li V**, *Development of engineered cementitious composites with limestone powder and blast furnace slag*, Materials & Structures, **43**(6), (2010), 803–814, DOI 10.1617/s11527-009-9549-0.

7 **Sahmaran M, Lachemi M, Hossain KMA, Ranade R, Li VC**, *Influence of aggregate type and size on ductility and mechanical properties of engineered cementitious composites*, ACI Materials Journal, **106**(3), (2009), 308–316.

8 **Lin YM, Wu H-C, Li VC**, *Development of flexural composite properties and dry shrinkage behavior of high-performance fiber reinforced cementitious composites at early ages*, ACI Materials Journal, **96**(1), (1999), 20–26.

9 **Felekoglu B, Tosun K, Baradan B**, *Effects of fiber type and matrix structure on the mechanical performance of self-compacting micro-concrete composites*, Cement and Concrete Research, **39**(11), (2009), 1023–1032, DOI 10.1016/j.cemconres.2009.07.007.

10 *ASTM C 348: Standard Test Method for Flexural Strength of Hydraulic-Cement Mortars*, ASTM International; 100 Barr Harbor Drive, PA, United States, 2002.

11 **Felekoglu B**, *High performance micro concrete design*, PhD thesis, Dokuz Eylul University; İzmir, Turkey, 2009.

12 *TS EN 197-1: Cement – Part 1: Composition, specification and conformity criteria for common cements*, Turkish Standards Institution; Ankara, Turkey, 2012.

13 *ASTM C 618: Standard Specification for Coal Fly Ash and Raw or Calcined Natural Pozzolan for Use in Concrete*, ASTM International; 100 Barr Harbor Drive, PA, United States, 2008.

14 *ASTM C 305: Standard Practice for Mechanical Mixing of Hydraulic Cement Pastes and Mortars of Plastic Consistency*, ASTM International; 100 Barr Harbor Drive, PA, United States, 1999.

15 **Soranakom C, Mobasher B**, *Correlation of tensile and flexural responses of strain softening and strain hardening cement composites*, Cement and Concrete Composites, **30**(6), (2008), 465–477, DOI 10.1016/j.cemconcomp.2008.01.007.

16 **Horikoshi T, Ogawa A, Saito T, Hoshiro H**, *Properties of Polyvinylalcohol fiber as reinforcing materials for cementitious composites*, Int'l RILEM Workshop on HPFRCC in Structural Application, In: **Fischer G, Li VC** (eds.), Proceedings of Int'l RILEM Workshop on HPFRCC in Structural Application, RILEM Publications SARL; RILEM, Bagneux, France, 2006, pp. 145–153.

17 **Oh BH, Shin KJ**, *Cracking, ductility and durability characteristics of HPFRCC with various mixture proportions and fibers*, Int'l RILEM Workshop on HPFRCC in Structural Application, In: **Fischer G, Li VC** (eds.), Proceedings of Int'l RILEM Workshop on HPFRCC in Structural Applica-

tion, RILEM Publications SARL; RILEM, Bagneux, France, 2006, pp. 213–222.

18 **Kunieda M, Rokugo K**, *Measurement of crack opening behavior within ECC under bending moment*, Int'l RILEM Workshop on HPFRCC in Structural Application, In: **Fischer G, Li VC** (eds.), Proceedings of Int'l RILEM Workshop on HPFRCC in Structural Application, RILEM Publications SARL; RILEM, Bagneux, France, 2006, pp. 313–322.

19 **Neville AM**, *Properties of Concrete Fourth and Final Edition*, Pearson; Prentice Hill, UK, 2000.

20 **Li VC**, *Durable Overlay Systems with Engineered Cementitious Composites (ECC)*, International Journal for Restoration of Buildings and Monuments, **9**(2), (2003), 1–20.

21 **Zhang J, Leung CKY, Cheung Y N**, *Flexural performance of layered ECC-concrete composite beam*, Composites Science and Technology, **66**(11-12), (2006), 1501–1512, DOI 10.1016/j.compscitech.2005.11.024.